Energy transport and optical line shapes in dimers: Analytical description of the influence of colored noise

Ch. Warns,[1] I. Barvik,[2] and P. Reineker[1]
[1]*Abteilung Theoretische Physik, Universität Ulm, Albert-Einstein-Allee 11, D-89069 Ulm, Germany*
[2]*Institute of Physics, Charles University, Ke Karlovu 5, 121–16 Prague, Czech Republic*
(Received 5 February 1997; revised manuscript received 22 December 1997)

For a dimer, i.e., the simplest molecular aggregate, the influence of local vibrations on the transport of electronic excitation energy and on the optical absorption line shape is investigated. The vibrations give rise to site energy fluctuations which are described by a dichotomic stochastic process with colored noise. The model includes also the limits of static and infinitely fast fluctuations. The equations of motion for the density matrix of the system and for the correlation functions describing the optical line shape are calculated analytically. The coherence of transport properties, the time dependence of the memory function of the generalized master equation, optical line shapes, and the connection between them are discussed. [S1063-651X(98)08204-4]

PACS number(s): 02.50.Ey, 05.30.−d

I. INTRODUCTION

The dynamics of a quantum particle, e.g., of an electron or an exciton, in organic molecular aggregates is the subject of many experimental and theoretical investigations in recent years. The interest in these investigations originates both from questions with respect to the fundamental understanding and with respect to potential applications, e.g., in nonlinear optics, molecular electronics, photonics, etc. One of the questions is whether the transport of the quantum particle occurs coherently in a wavelike manner or incoherently via a hopping process. The answer to this question is fundamental for the understanding of luminescence in organic materials or for the description of energy transfer in photosynthetic light harvesting systems. With the development of femtosecond laser spectroscopy new experimental information is available which might help to elucidate this question.

From the theoretical point of view the coherence or incoherence of the quantum particle transport is strongly influenced by its interaction with vibrational degrees of freedom. To describe this interaction, several models have been developed (for references see [1,2]). In these models it is assumed that at low temperatures the particle moves coherently in a wavelike manner according to the Schrödinger equation. With increasing temperature the coherence of the wave is disturbed by the interaction with vibrational degrees of freedom and the transport occurs via a hopping process which is described by a master equation or in the continuum limit by a diffusion equation. A fully quantum mechanical approach to this transport problem was performed on the basis of the density operator equation together with projection techniques resulting in a generalized master equation [3–5], or based on Green's function techniques [6]. In another approach the vibrational degrees of freedom were considered as classical variables giving rise to fluctuations of the local excitation energies and of the transfer matrix elements. The excitation energies and transfer matrix elements were treated as independent Gaussian stochastic processes with white noise [7–9], which is a reasonable assumption at not too low temperatures. This model was quite successful in the description of a series of experimental situations such as optical absorption, spin resonance, or quantum particle transport (for references see [2]). A straightforward generalization of this model, performed in recent years, is the replacement of the white noise processes by colored noise with exponentially decaying correlation functions [10–16]. This generalization makes the model considerably richer, because it allows for fluctuations on all time scales including the static and white noise limits. At the same time the equations become more complicated and up to now also in the case of dichotomic colored noise in dimers only numerical solutions of the transport problem were obtained. In this paper we present an analytical description of energy transfer and optical absorption in dimers when the influence of the vibrational degrees of freedom is described by dichotomic colored noise. The paper is organized as follows: Section II explains the model, in Sec. III the dynamics of the system is derived, Sec. IV derives the memory function of the generalized master equation, and Sec. V presents its optical properties. In the conclusion (Sec. VI) the connection between transport and optical line shape is discussed.

II. MODEL FOR EXCITONIC DYNAMICS

In our description of exciton dynamics we start from a Hamiltonian which consists of a time independent and a stochastically time dependent part:

$$H = H_0 + H_1(t), \tag{1}$$

$$H_0 = \sum_m \epsilon_n a_n^\dagger a_n + \sum_{n \neq m} J_{nm} a_n^\dagger a_m, \tag{2}$$

$$H_1(t) = \sum_n \epsilon_n(t) a_n^\dagger a_n + \sum_{n \neq m} J_{nm}(t) a_n^\dagger a_m. \tag{3}$$

Here $a_n^\dagger$ and a_n are creation and annihilation operators for an excitation at site n, ϵ_n is the local excitation energy, and J_{nm} is the electronic transfer matrix element between sites m and n. $H_1(t)$ in Eq. (3) describes the influence of the phonon bath via fluctuations of the excitation energy $[\epsilon_n(t)]$ and of

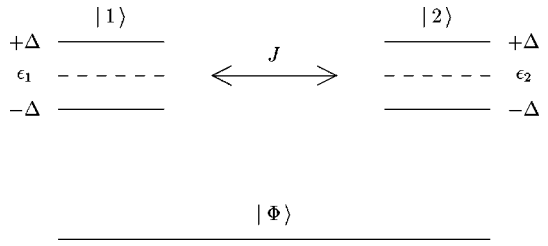

FIG. 1. Parameters of the model.

the transfer matrix element $[J_{nm}(t)]$. Different types of stochastic processes can be used here for $\epsilon_n(t)$ and $J_{nm}(t)$, but most of them introduce the need for some kind of approximation to compute the exciton density or the optical absorption spectra.

To simplify the treatment as far as possible, we allow only fluctuations of the local excitation energies $\epsilon_n(t)$ and describe them by independent dichotomic stochastic processes with exponentially decaying correlation functions. In this model the time dependent variables assume only two values, $\epsilon_n(t)=\pm\Delta$, with a switching rate λ corresponding to a correlation time $\tau=1/\lambda$. The process is characterized by the following equations:

$$\langle \epsilon_n(t)\rangle = 0, \tag{4}$$

$$\langle \epsilon_m(t)\epsilon_n(t')\rangle = \delta_{nm}\Delta^2 e^{-\lambda|t-t'|}, \tag{5}$$

$$\langle \epsilon(t_1)\epsilon(t_2)\cdots\epsilon(t_{2\mu-1})\rangle = 0, \tag{6}$$

$$\langle \epsilon(t_1)\epsilon(t_2)\cdots\epsilon(t_{2\mu})\rangle = \langle \epsilon(t_1)\epsilon(t_2)\rangle\cdots\langle \epsilon(t_{2\mu-1})\epsilon(t_{2\mu})\rangle, \tag{7}$$

$$t_1 \geqslant t_2 \geqslant \cdots \geqslant t_{2\mu},$$

i.e., stochastic processes at different sites are independent, the average value of the fluctuations vanishes, two-time correlation functions decay exponentially, and multitime correlation functions are calculated according to Eqs. (6) and (7). The Fourier transform of this noise process is a Lorentzian, so the bandwidth is limited. This process also contains the limiting cases of static disorder with $\lambda=0$, of motional narrowing with Δ finite and $\lambda\to\infty$, and the white noise limit. The latter is obtained with $\lambda\to\infty$ and $\Delta\to\infty$ but keeping $\gamma_0=\Delta^2/\lambda$ finite, so that $\Delta^2 e^{-\lambda|t-t'|}\to\gamma_0\delta(t-t')$, which is the correlation function of the white noise process.

III. ENERGY TRANSPORT

In the following we discuss a symmetric dimer ($\epsilon_1=\epsilon_2$) as the simplest case of a molecular aggregate, and take into account energy fluctuations only at the two sites 1 and 2. In Fig. 1, $|\Phi\rangle$ is the electronic ground state and $|n\rangle$ describes an electronic excitation localized at site n. J is the transfer matrix element. The transport of the electronic excitation between the two sites can be described with the density operator ρ, which obeys the following equation ($\hbar=1$):

$$\dot{\rho} = -i[H(t),\rho]. \tag{8}$$

In this paper we assume that the electronic excitation of the dimer does not decay. Then the density operator ρ has four matrix elements, the diagonal elements ρ_{nn} describing the occupation probability at site n, and nondiagonal elements ρ_{nm} containing phase relations between sites n and m. The equations of motion for these matrix elements read

$$\dot{\rho}_{11} = iJ\rho_{12} - iJ\rho_{21}, \tag{9}$$

$$\dot{\rho}_{22} = iJ\rho_{21} - iJ\rho_{12}, \tag{10}$$

$$\dot{\rho}_{12} = iJ\rho_{11} - iJ\rho_{22} - i\epsilon_1(t)\rho_{12} + i\epsilon_2(t)\rho_{12}, \tag{11}$$

$$\dot{\rho}_{21} = iJ\rho_{22} - iJ\rho_{11} + i\epsilon_1(t)\rho_{21} - i\epsilon_2(t)\rho_{21}. \tag{12}$$

Because of the presence of stochastically time dependent variables in this set of differential equations, one has to consider the averaged matrix elements $\langle\rho_{ij}\rangle$. But averaging Eqs. (9)–(12) yields additional unknowns like $\langle\epsilon_1(t)\rho_{12}\rangle$, so that the set of equations is no longer closed. Additional equations for these elements can be obtained using a theorem by Shapiro and Loginov [17]:

$$\frac{d}{dt}\langle \epsilon(t)F_t[\epsilon]\rangle = \left\langle \epsilon(t)\frac{d}{dt}F_t[\epsilon]\right\rangle - \lambda\langle \epsilon(t)F_t[\epsilon]\rangle, \tag{13}$$

with $F_t[\epsilon]$ being a functional of the stochastic variable $\epsilon(t)$. For the stochastic average $\langle\epsilon_1(t)\rho_{12}\rangle$, e.g., the differential equation is

$$\frac{d}{dt}\langle \epsilon_1(t)\rho_{12}\rangle = \langle \epsilon_1(t)\dot{\rho}_{12}\rangle - \lambda\langle \epsilon_1(t)\rho_{12}\rangle, \tag{14}$$

which, using Eq. (5) and (11), results in

$$\frac{d}{dt}\langle \epsilon_1(t)\rho_{12}\rangle = -i\Delta^2\langle\rho_{12}\rangle + i\langle \epsilon_1(t)\epsilon_2(t)\rho_{12}\rangle - \lambda\langle \epsilon_1(t)\rho_{12}\rangle + iJ\langle \epsilon_1(t)\rho_{11}\rangle - iJ\langle \epsilon_1(t)\rho_{22}\rangle. \tag{15}$$

On the right side we have the new quantity $\langle\epsilon_1(t)\epsilon_2(t)\rho_{12}\rangle$. Using the theorem of Shapiro and Loginov again,

$$\frac{d}{dt}\langle \epsilon_i(t)\epsilon_k(t)F_t[\epsilon]\rangle = \left\langle \epsilon_i(t)\epsilon_k(t)\frac{d}{dt}F_t[\epsilon]\right\rangle - 2\lambda\langle \epsilon_i(t)\epsilon_k(t)F_t[\epsilon]\rangle, \tag{16}$$

we get for the quantity under discussion

$$\frac{d}{dt}\langle \epsilon_1(t)\epsilon_2(t)\rho_{12}\rangle = \langle \epsilon_1(t)\epsilon_2(t)\dot{\rho}_{12}\rangle - 2\lambda\langle \epsilon_1(t)\epsilon_2(t)\rho_{12}\rangle. \tag{17}$$

For most types of stochastic processes, this expansion leads to an infinite set of equations, which can only be solved by introducing some sort of approximation. However, inserting $\dot{\rho}_{12}$ from Eq. (11) and using Eqs. (4)–(7), for the dichotomic process we arrive at a closed set of coupled differential equations. In matrix form, these equations read

$$\dot{\varrho} = L_{16}\varrho, \tag{18}$$

where ϱ is a 16-dimensional column vector and L_{16} a 16-dimensional non-Hermitian matrix, with the following vector notation for the components of ϱ:

$$\varrho_1=\langle\rho_{11}\rangle, \quad \varrho_9=\langle\epsilon_1(t)\rho_{11}\rangle,$$

$$\varrho_2=\langle\rho_{22}\rangle, \quad \varrho_{10}=\langle\epsilon_1(t)\rho_{22}\rangle,$$

$$\varrho_3=\langle\rho_{12}\rangle, \quad \varrho_{11}=\langle\epsilon_2(t)\rho_{11}\rangle,$$

$$\varrho_4=\langle\rho_{21}\rangle, \quad \varrho_{12}=\langle\epsilon_2(t)\rho_{22}\rangle,$$

$$\varrho_5=\langle\epsilon_1(t)\rho_{12}\rangle, \quad \varrho_{13}=\langle\epsilon_1(t)\epsilon_2(t)\rho_{12}\rangle,$$

$$\varrho_6=\langle\epsilon_1(t)\rho_{21}\rangle, \quad \varrho_{14}=\langle\epsilon_1(t)\epsilon_2(t)\rho_{21}\rangle,$$

$$\varrho_7=\langle\epsilon_2(t)\rho_{12}\rangle, \quad \varrho_{15}=\langle\epsilon_1(t)\epsilon_2(t)\rho_{22}\rangle,$$

$$\varrho_8=\langle\epsilon_2(t)\rho_{21}\rangle, \quad \varrho_{16}=\langle\epsilon_1(t)\epsilon_2(t)\rho_{11}\rangle.$$

The matrix L_{16} of the system of differential equations (18) $\dot{\varrho}=L_{16}\varrho$ reads (vanishing matrix elements are represented by a dot)

$$\begin{pmatrix}
. & . & iJ & -iJ & . & . & . & . & . & . & . & . & . & . & . & . \\
. & . & -iJ & iJ & . & . & . & . & . & . & . & . & . & . & . & . \\
iJ & -iJ & . & . & -i & . & i & . & . & . & . & . & . & . & . & . \\
-iJ & iJ & . & . & . & i & . & -i & . & . & . & . & . & . & . & . \\
. & . & -i\Delta^2 & . & -\lambda & . & . & . & iJ & -iJ & . & . & i & . & . & . \\
. & . & . & i\Delta^2 & . & -\lambda & . & . & -iJ & iJ & . & . & . & -i & . & . \\
. & . & i\Delta^2 & . & . & . & -\lambda & . & . & . & iJ & -iJ & -i & . & . & . \\
. & . & . & -i\Delta^2 & . & . & . & -\lambda & . & . & -iJ & iJ & . & i & . & . \\
. & . & . & . & iJ & -iJ & . & . & -\lambda & . & . & . & . & . & . & . \\
. & . & . & . & -iJ & iJ & . & . & . & -\lambda & . & . & . & . & . & . \\
. & . & . & . & . & . & iJ & -iJ & . & . & -\lambda & . & . & . & . & . \\
. & . & . & . & . & . & -iJ & iJ & . & . & . & -\lambda & . & . & . & . \\
. & . & . & . & i\Delta^2 & . & -i\Delta^2 & . & . & . & . & . & -2\lambda & . & -iJ & iJ \\
. & . & . & . & . & -i\Delta^2 & . & i\Delta^2 & . & . & . & . & . & -2\lambda & iJ & -iJ \\
. & . & . & . & . & . & . & . & . & . & . & . & -iJ & iJ & -2\lambda & . \\
. & . & . & . & . & . & . & . & . & . & . & . & iJ & -iJ & . & -2\lambda
\end{pmatrix}$$

(The matrix for the case containing also fluctuations of J_{nm} can be found in Appendix A of [15]).

With the ansatz $\varrho(t)=ve^{Rt}$, the differential equations transform to a non-Hermitian eigenvalue problem for the eigenvalues R_n and eigenvectors v^n of the matrix L_{16}. The structure of this matrix is such that its eigensolutions can be obtained [16] using computer algebra (MAPLE [18]). We introduce the scaled model parameters λ_s,Δ_s and scaled eigenvalues R_{sn} by

$$R_{sn}=\frac{R_n}{2J}, \quad \lambda_s=\frac{\lambda}{2J}, \quad \Delta_s=\frac{\Delta}{2J}. \tag{19}$$

The eigenvalues are then given by

$$R_{s1}=0,$$

$$R_{s2}=-2\lambda_s,$$

$$R_{s3},\ldots,R_{s6}=-\lambda_s,$$

$$R_{s7},R_{s8}=-\lambda_s\pm i,$$

$$R_{s9},\ldots,R_{s12}=-\lambda_s\pm\frac{1}{\sqrt{2}}\sqrt{\lambda_s^2-4\Delta_s^2-1\pm\sqrt{16\Delta_s^4-8\lambda_s^2\Delta_s^2+8\Delta_s^2+\lambda_s^4+2\lambda_s^2+1}},$$

$$R_{s13},\ldots,R_{s16}=-\lambda_s\pm\sqrt{\lambda_s^2-1-2\Delta_s^2\pm2\sqrt{\Delta_s^4-\lambda_s^2}}, \tag{20}$$

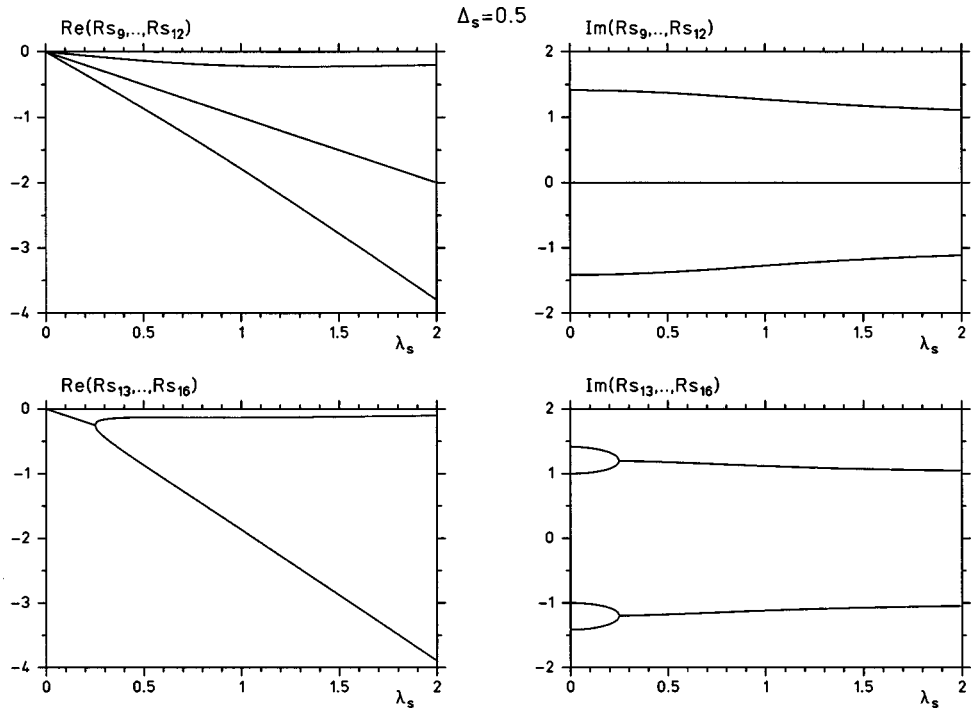

FIG. 2. Real and imaginary part of $R_{s9}, \ldots, R_{s16}$ for $\Delta_s = 0.5$.

with the following choices for the signs: $R_{s9}\,(++)$, $R_{s10}\,(+-)$, $R_{s11}\,(-+)$, $R_{s10}\,(--)$, and correspondingly for $R_{s13}, \ldots, R_{s16}$. Using these eigenvalues, analytical expressions for the eigenvectors v^n can also be obtained [19].

Figures 2 and 3 show the real and imaginary parts of the eigenvalues for $\Delta_s = 0.5$ and $\Delta_s = 2$ as a function of λ_s. In both cases the eigenvalues $R_{s1}, \ldots, R_{s6}$ and R_{s9}, R_{s10} are purely real and the eigenvalues R_{s7}, R_{s8}, R_{s11}, R_{s12} are always complex. The behavior of the eigenvalues $R_{s13}, \ldots, R_{s16}$ is more complicated: (1) for $\Delta_s = 0.5$, e.g., all four are complex for all values of λ_s; (2) in the case of $\Delta_s = 2$ two of them are purely real between $\lambda_s = \sqrt{17/(7+4\sqrt{2})}$ and $\lambda_s = \sqrt{17/(7-4\sqrt{2})}$; and (3) between $\lambda_s = \sqrt{17/(7-4\sqrt{2})}$ and $\lambda_s = 4.0$ all four are real.

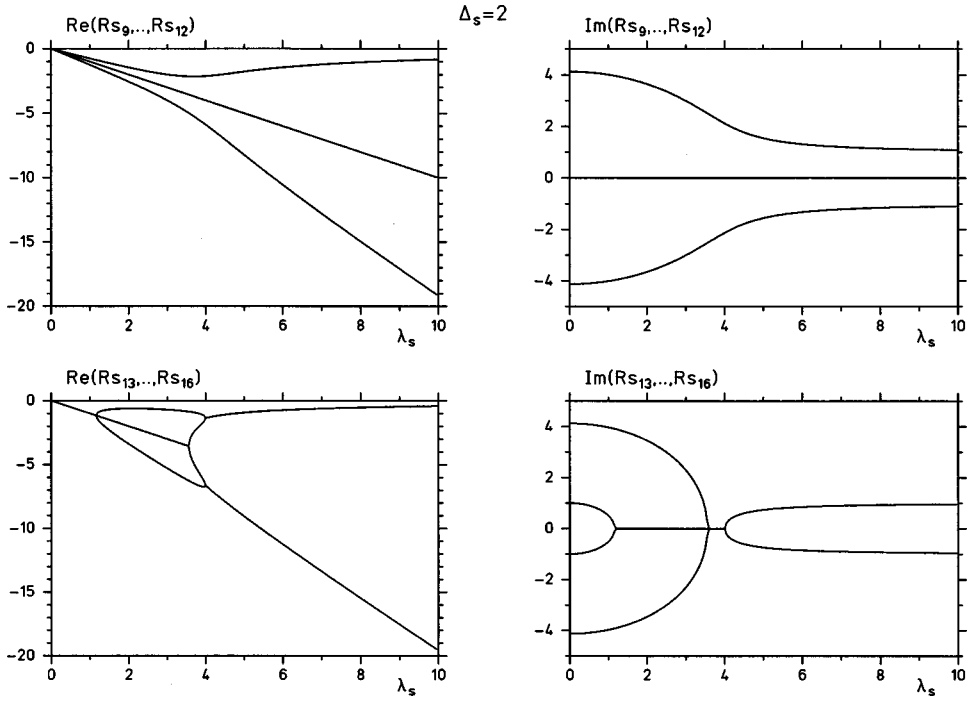

FIG. 3. Real and imaginary part of $R_{s9}, \ldots, R_{s16}$ for $\Delta_s = 2.0$.

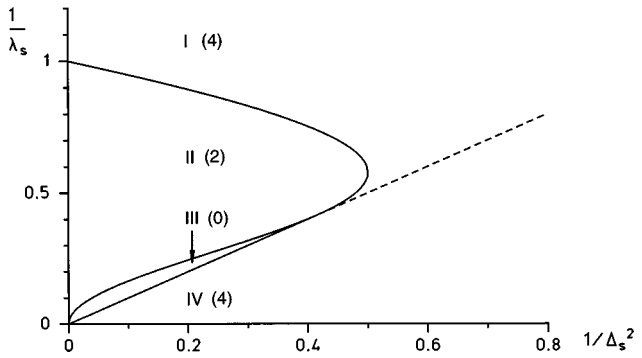

FIG. 4. Number of complex eigenvalues $R_{s13},\ldots,R_{s16}$ in the $1/\lambda_s-1/\Delta_s$ plane.

Figure 4 shows the areas in the λ_s^{-1}-Δ_s^{-2} plane, where four, two, and none of the four eigenvalues $R_{s13},\ldots,R_{s16}$ are complex (indicated by the numbers in the brackets in Fig. 4). With the notation $x=\Delta_s^{-2}$, $y=\lambda_s^{-1}$ the borderlines between the four areas are given by the curves

$$y=x, \tag{21}$$

$$y=\frac{\sqrt{2-x+2\sqrt{1-2x}}}{\sqrt{x+4}}, \tag{22}$$

$$y=\frac{\sqrt{2-x-2\sqrt{1-2x}}}{\sqrt{x+4}}. \tag{23}$$

The straight line determines the vanishing of the radicand of the inner square root, the curves of Eqs. (22) and (23) the vanishing of the radicand of the outer square roots. From this discussion we expect two areas of coherent motion: area I for small values of λ_s, corresponding to the (quasi) static case, and area IV for large values of λ_s, corresponding to the case of fast fluctuations.

The general solution for the differential equation (18) is given by the superposition of the eigensolutions

$$\varrho(t)=\sum_{i=1}^{16} c_i v^i \exp(R_i t). \tag{24}$$

A closer inspection of the eigenvectors v shows that only the eigensolutions $v^i\exp(R_i t)$ with $i=1,3,13,\ldots,16$ contribute to the first element of ϱ, which is the probability $\langle\rho_{11}\rangle=P_1(t)$ of finding the excitation at site 1. The dynamics of $P_1(t)$ are therefore determined by the eigenvalues R_{s1} and R_{s3}, which are purely real, and by $R_{s13},\ldots,R_{s16}$ which — as discussed above — may be real or complex depending on the magnitudes of λ_s and Δ_s. The coefficients c_i are determined by the initial conditions for the density operator $\rho(t=0)$ and are evaluated using the left eigenvectors of the non-Hermitian matrix L_{16}. As initial conditions we have used a density matrix with $\rho_{11}(0)=1$ and all other matrix elements zero. The analytic expression for $P_1(t)=\langle\rho_{11}(t)\rangle$ is rather involved and not presented explicitly in this paper [19].

The left column of Fig. 5 shows the time evolution of $\langle\rho_{11}\rangle$ for $\Delta_s=0.5$, i.e., $\Delta_s^{-2}=4$ and various values of λ_s. We see that for all values of λ_s the occupation probability $P_1(t)$ shows an oscillatory behavior. For small λ_s values the probability oscillates with two frequencies, for large λ_s only a single frequency survives.

In Fig. 6 for $\Delta_s=2$, i.e., $\Delta_s^{-2}=0.25$, the series of λ_s values shows the time dependence of occupation probabilities starting in region I, crossing II and III, and ending in region IV. The left column starts with an occupation probability oscillating with two frequencies (region I). For intermediate values of λ_s the probability decays exponentially, and for large λ_s values it oscillates with a single frequency. A corresponding behavior is shown by the time evolution of $\langle\rho_{12}\rangle$ (center column in Figs. 5 and 6), describing phase relations between the two sites, whose dynamics is determined additionally by the eigenvalues $R_{s9},\ldots,R_{s12}$.

In the static case with $\lambda_s=0$, all real parts of the eigenvalues vanish, and the imaginary parts become ±1 and $\pm\sqrt{4\Delta_s^2+1}$, which corresponds to undamped oscillations of the electronic excitation between the sites 1 and 2, with the two frequencies $2J$ and $2\sqrt{\Delta^2+J^2}$, as expected from the solution of the Schrödinger equation in the four possible configurations $\epsilon_1=\epsilon_2=\pm\Delta$ and $\epsilon_1=-\epsilon_2=\pm\Delta$.

In the fast modulation case with $\lambda_s\to\infty$, all imaginary parts tend to $\pm i$, so that only one oscillation frequency survives, which also becomes undamped:

$$\lim_{\lambda_s\to\infty} R_{s13}=i, \quad \lim_{\lambda_s\to\infty} R_{s14}=-2\lambda_s-i,$$

$$\lim_{\lambda_s\to\infty} R_{s15}=-i, \quad \lim_{\lambda_s\to\infty} R_{s16}=-2\lambda_s+i.$$

The white noise limit can be obtained after substituting Δ_s^2 by $\lambda_s\gamma_0'$ ($\gamma_0'=\gamma_0/2J$) and then evaluating the asymptotics of the eigenvalues for $\lambda_s\to\infty$ (γ_0' finite):

$$\lim_{\lambda_s\to\infty} R_{s13}=-\gamma_0'+\sqrt{\gamma_0'^2-1}\ , \quad \lim_{\lambda_s\to\infty} R_{s14}=-\infty,$$

$$\lim_{\lambda_s\to\infty} R_{s15}=-\gamma_0'-\sqrt{\gamma_0'^2-1}\ , \quad \lim_{\lambda_s\to\infty} R_{s16}=-\infty.$$

From R_{s13} and R_{s15} we see that the excitation transport is coherent if $\gamma_0'<1$ ($\gamma_0<2J$) and incoherent in the opposite case [2,8].

IV. MEMORY FUNCTIONS OF THE GENERALIZED MASTER EQUATION

Up to now we have described the exciton transport in terms of the density operator formalism. An alternative approach is given by the generalized master equation (GME) [1,2] for the site occupation probabilities, i.e., by the diagonal elements of the density operator $P_n(t)=\langle\rho_{nn}\rangle$. The generalized master equation is given by

$$\partial P_m(t)/\partial t=\sum_{n(\neq m)}\int_0^t [w_{mn}(t-\tau)P_n(\tau) - w_{nm}(t-\tau)P_m(\tau)]d\tau \tag{25}$$

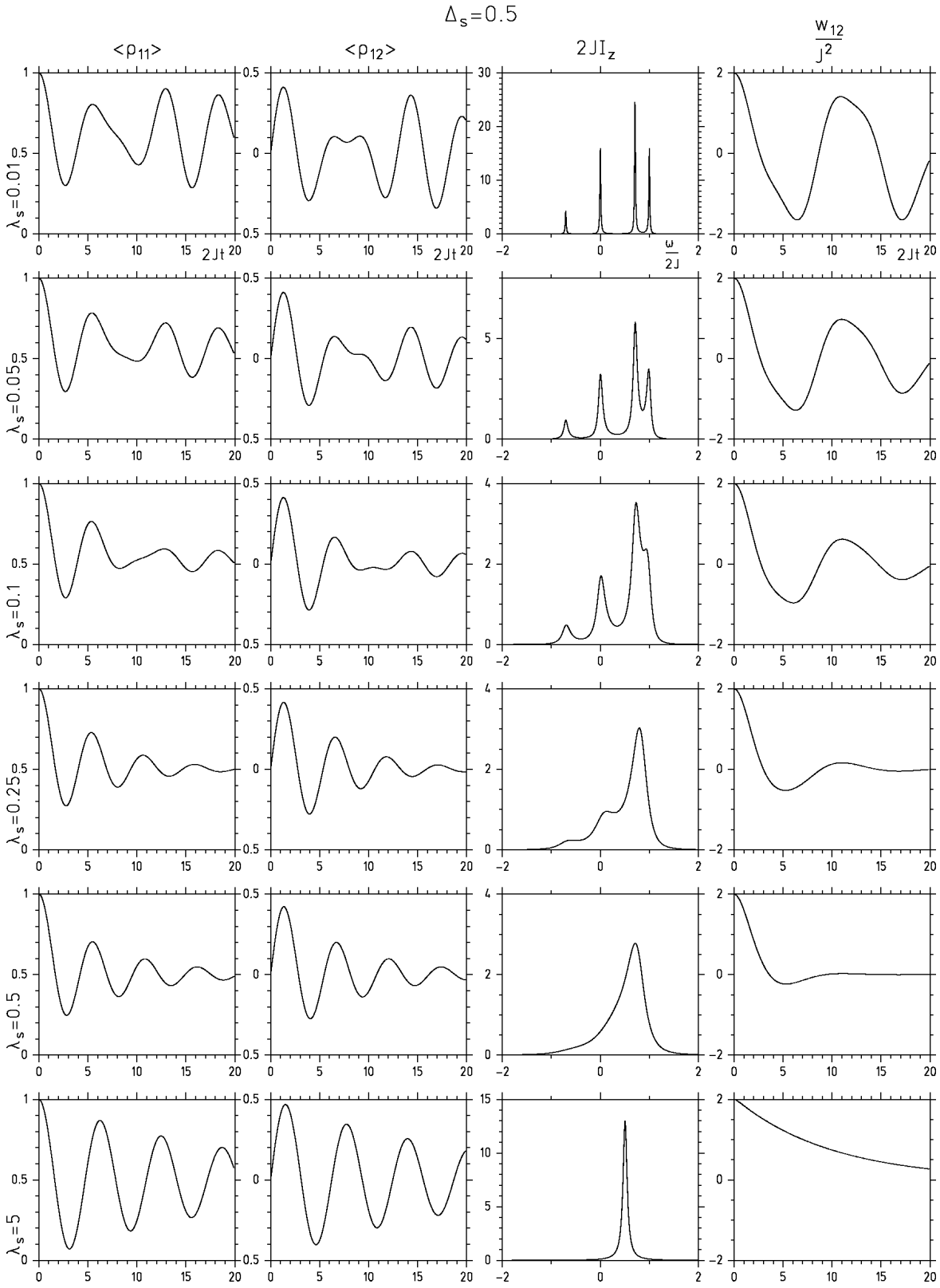

FIG. 5. Excitation transport, optical absorption, and memory function for $\Delta_s = 0.5$.

and the dynamics of the system is determined by the memory function $w_{mn}(t)$. In the case of a dimer and assuming that the excitation is initially located at site 1, the Laplace transform of the GME reads

$$s\tilde{P}_1(s) - 1 = -\tilde{w}_{12}(s)[\tilde{P}_1(s) - \tilde{P}_2(s)], \tag{26}$$

$$s\tilde{P}_2(s) = -\tilde{w}_{21}(s)[\tilde{P}_2(s) - \tilde{P}_1(s)]. \tag{27}$$

From the analytical solution for $P_1(t)$ [19] obtained with MAPLE we get for the Laplace transform

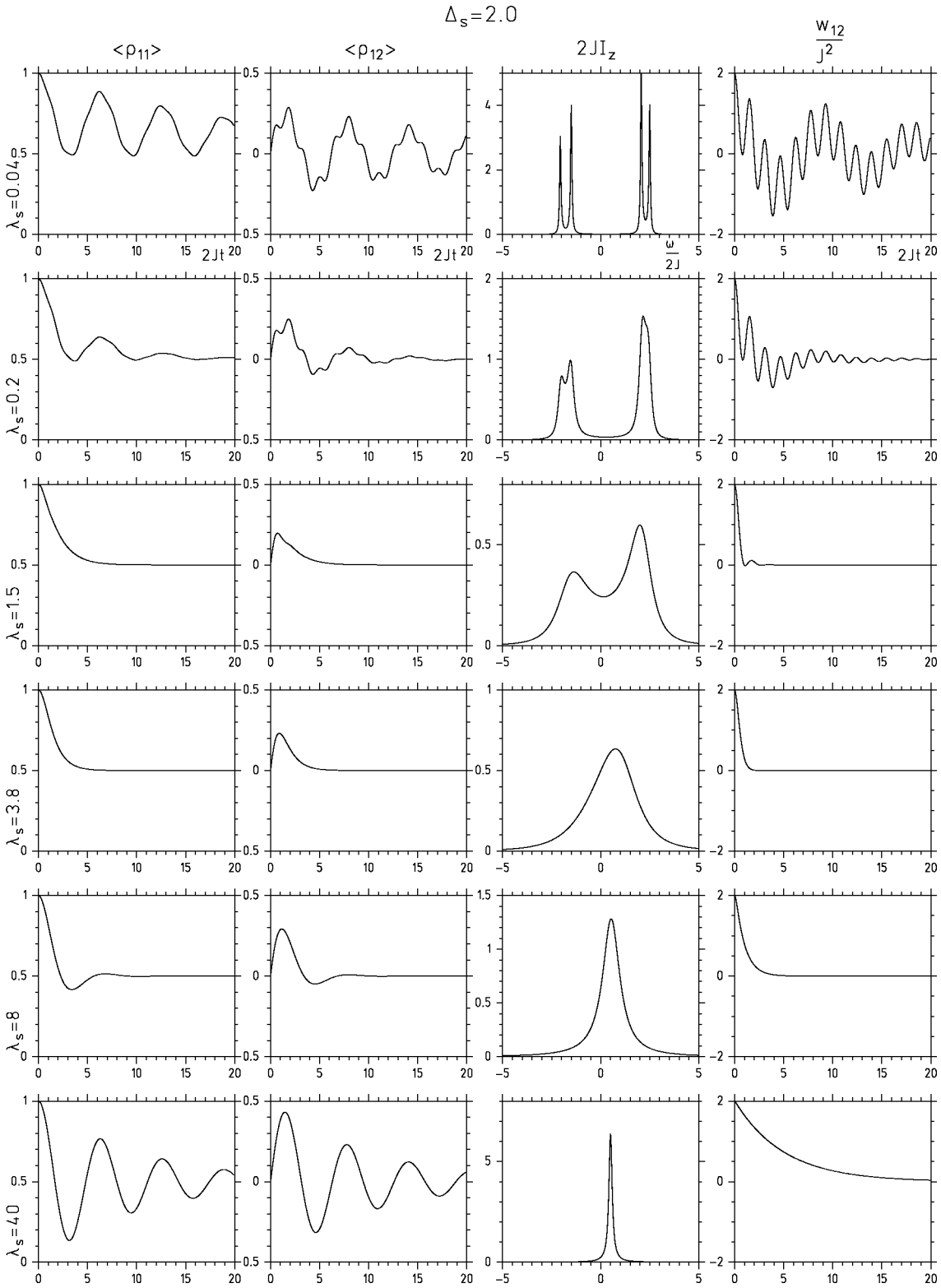

FIG. 6. Excitation transport, optical absorption, and memory function for $\Delta_s=2$.

$$\widetilde{P}_1(s)=\frac{s^5+5s^4\lambda+(4\Delta^2+6J^2+8\lambda^2)s^3+(12\Delta^2\lambda+4\lambda^3+14\lambda J^2)s^2}{s(s-R_{13})(s-R_{14})(s-R_{15})(s-R_{16})}$$
$$+\frac{(8J^4+12J^2\Delta^2+16\lambda^2J^2+8\Delta^2\lambda^2)s+8J^4\lambda+8\lambda^3J^2+8J^2\Delta^2\lambda}{s(s-R_{13})(s-R_{14})(s-R_{15})(s-R_{16})}. \tag{28}$$

Solving Eq. (26) or Eq. (27) for $\widetilde{w}_{12}(s)$ yields

$$\tilde{w}_{12}(s)=\tilde{w}_{21}(s)=\frac{[2s^3+10\lambda s^2+2(2\Delta^2+8\lambda^2+4J^2)s+8\Delta^2\lambda+8\lambda^3+8J^2\lambda]J^2}{s^4+5\lambda s^3+(4J^2+8\lambda^2+4\Delta^2)s^2+(12\Delta^2\lambda+4\lambda^3+4J^2\lambda)s+8\Delta^2\lambda^2+8\Delta^2J^2}. \tag{29}$$

The time development of the memory function is obtained by performing the inverse Laplace transform

$$w_{12}(t)=w_{21}(t)=\sum_i f_i \exp(r_i t)=\sum_i \frac{[2r_i^3+10\lambda r_i^2+(4\Delta^2+16\lambda^2+8J^2)r_i+8\Delta^2\lambda+8\lambda^3+8J^2\lambda]J^2}{4r_i^3+15\lambda r_i^2+(8J^2+16\lambda^2+8\Delta^2)r_i+12\Delta^2\lambda+4\lambda^3+4J^2\lambda}\exp(r_i t), \tag{30}$$

where the r_i are the solutions of the zeros of Eq. (29).

The time dependence of the memory function is shown in the right column of Figs. 5 and 6. As essential feature we observe damped oscillations. A more detailed investigation shows that the oscillations are the result of the discrete energy fluctuations of the dichotomic process and the exponential decay of the memory function is responsible for the transition from coherent to incoherent exciton motion. The decay time of the memory function is related to the time constant for the loss of coherence of the exciton transport.

V. OPTICAL ABSORPTION

In the framework of linear response theory the optical absorption line shape of the dimer is given by

$$I(\omega)=\mathrm{Re}\int_0^\infty e^{i\omega t}\langle\mu(t)\mu(0)\rangle dt. \tag{31}$$

$\mu(t)$ is the optical dipole operator. It can be expressed by the creation and annihilation operators for a local excitation and the transition dipole moment μ_n at site n in the following way:

$$\mu(t)=\sum_n \mu_n[a_n^\dagger(t)+a_n(t)]. \tag{32}$$

We assume that only the ground state $|\Phi\rangle$ is populated in thermal equilibrium and that the μ_n are independent of the site index n and oriented parallel to the z direction. For the normalized line shape $\tilde{I}_z(\omega)$ we get

$$\tilde{I}_z(\omega)=\frac{1}{\pi}\sum_{m,n}\mathrm{Re}\int_0^\infty e^{i\omega t}U_{mn}(t)dt=\frac{1}{\pi}\mathrm{Re}\int_0^\infty e^{i\omega t}S(t)dt$$
$$=\frac{1}{\pi}\mathrm{Re}\tilde{S}(\omega). \tag{33}$$

Here $U(t)=\overleftarrow{T}\exp[-\int_0^t dt' H(t')]$ describes the time evolution of the system, $U_{mn}(t)$ are the matrix elements $\langle m|U(t)|n\rangle$, and $S(t)$ is defined below. To simplify the calculation we introduce the variables

$$x=U_{11}+U_{12},\quad y=U_{21}+U_{22}, \tag{34}$$

$$S(t)=\langle x+y\rangle,$$

$$A(t)=\langle\epsilon_1 x\rangle+\langle\epsilon_2 y\rangle,$$

$$B(t)=\langle\epsilon_2 x\rangle+\langle\epsilon_1 y\rangle,$$

$$C(t)=\langle\epsilon_1\epsilon_2 x\rangle+\langle\epsilon_1\epsilon_2 y\rangle. \tag{35}$$

The equations of motion for these quantities can be derived using again the theorem of Shapiro and Loginov and are given by

$$\frac{d}{dt}\begin{pmatrix}S(t)\\A(t)\\B(t)\\C(t)\end{pmatrix}=\begin{pmatrix}-iJ & -i & 0 & 0\\ -i\Delta^2 & -\lambda & -iJ & 0\\ 0 & -iJ & -\lambda & -i\\ 0 & 0 & -i\Delta^2 & -2\lambda-iJ\end{pmatrix}\begin{pmatrix}S(t)\\A(t)\\B(t)\\C(t)\end{pmatrix}. \tag{36}$$

The line shape is obtained by Laplace transforming the equations of motion and solving for $\tilde{S}(\omega_s)$ ($\omega_s=\omega/2J$). We arrive at the following finite continued fraction:

$$\tilde{S}(\omega_s)2J=2[-i(\omega_s-\tfrac{1}{2})+\Delta_s^2(-i\omega_s+\lambda_s+\tfrac{1}{4}\{-i\omega_s+\lambda_s$$
$$+\Delta_s^2[-i(\omega_s-\tfrac{1}{2})+2\lambda_s]^{-1}\}^{-1})^{-1}]^{-1}. \tag{37}$$

The optical line shape can also be calculated from the density operator ρ by supplementing the Hilbert space by the ground state $|\Phi\rangle$ of the dimer, giving additional matrix elements ρ_{0n} and ρ_{n0}. The eigenvalue equation for the density operator then factorizes into a part describing the transport and a part describing the optical absorption. Therefore, as in the case of white noise, the two phenomena are mathematically independent.

The line shape for $\Delta_s=0.5$ and various values of λ_s is shown in Fig. 5 in the right column. For small values of λ_s we obtain a strongly structured line; the position of the peaks is determined by the random energy distribution $\epsilon\pm\Delta_s$, on account of the quasistatic dichotomic noise, and the strength of the transfer matrix element (compare the following paragraph), and their widths by the lifetime of the energy state, i.e., by λ_s. With increasing values of λ_s the lines become broader and merge. For very large values of λ_s and finite values of Δ_s the lines show a narrowing, because the fluctuations are now so fast that the electronic degrees of freedom can no longer follow. In Fig. 6 the third column represents optical line shapes for $\Delta_s=2$. For small values of λ_s we have a line shape whose structure is determined by the quasistatic energy distributions. With increasing λ_s the peaks become broader and merge and for large values of the switching rate we have again a dynamically narrowed line.

In the static case with $\lambda_s=0$, the optical absorption energies correspond to the Davydov splitting at the four possible

energy combinations $\epsilon_1=\epsilon_2=\pm\Delta$ and $\epsilon_1=-\epsilon_2=\pm\Delta$, giving rise to absorption at the frequencies $\pm\Delta+J$ and $\pm\Gamma$ ($\Gamma=\sqrt{\Delta^2+J^2}$):

$$\tilde{I}_z(\omega)=\frac{1}{6}\Bigg[\delta(\omega-(\Delta+J))+\delta(\omega-(-\Delta+J)) +2\left(1+\frac{J}{\Gamma}\right)\delta(\omega-\Gamma)+2\left(1-\frac{J}{\Gamma}\right)\delta(\omega+\Gamma)\Bigg]. \tag{38}$$

In the fast modulation case with $\lambda_s\to\infty$, the line shape becomes peaked at $\omega_s=1/2$, i.e., $\omega=J$,

$$\tilde{S}(\omega)=\frac{2}{-i(\omega-J)}. \tag{39}$$

The white noise limit can be obtained again by substitution of Δ_s^2 with $\lambda_s\gamma_0'$ ($\gamma_0'=\gamma_0/2J$) and evaluating the limit of $\tilde{S}(\omega_s)$ for $\lambda_s\to\infty$,

$$\tilde{I}_z(\omega)=\frac{1}{\pi}\frac{\gamma_0}{\gamma_0^2+(\omega-J)^2}. \tag{40}$$

The linewidth at half maximum is given by $2\gamma_0$.

VI. CONCLUSION

Figure 5 shows that for small amplitudes of the energy fluctuations $\Delta_s=0.5$ the excitation energy transport in the dimer shows damped oscillations for all values of λ_s and thus this transport can be denoted as coherent in the whole λ_s range. For the larger fluctuation amplitude in Fig. 6 we have two transitions between coherent and incoherent transport. The first corresponds to the transition between regions I and II in Fig. 1, the second to the transition into region IV. In the white noise case only the second transition is present.

In the third columns in Figs. 5 and 6 the optical line shapes are pictured for the same values of the model parameter. For slow fluctuations we have the line shape corresponding to the quasistatic distribution of energy levels, i.e., an inhomogeneously broadened line. For fast fluctuations the line shows dynamic narrowing and a homogeneous width. Thus the model allows us to describe a continuous transition between inhomogeneously and homogeneously broadened lines.

Comparing the transport and the optical line shapes, we see an oscillatory behavior of the occupation probabilities when the optical line shape is narrow both in the inhomogeneous and homogeneous limits. When the full half-width of the line is equal to $4J$ (in the scaled units we are using this corresponds to a half-width of 2), the occupation probability decays without oscillations to the stationary value. Such a situation occurs in Fig. 6, but not in Fig. 5.

As regards the memory function, its decay constant passes through a maximum with increasing values of λ_s. For $\Delta_s=0.5$ the largest decay constant is obtained for $\lambda_s=0.5$ and in this case the oscillations in the exciton transport decay fastest. In the case of Fig. 6 the decay constant of the memory function increases up to $\lambda_s=1.5$ and decreases again. This fast memory loss shows in the absence of oscillations in the occupation probability for $\lambda_s=1.5$ and 3.8. We plan to give a detailed discussion of the behavior of the memory function in the future.

ACKNOWLEDGMENTS

The support of the Deutscher Akademischer Austauschdienst (DAAD), of the Volkswagen Foundation, and of the Deutsche Forschungsgemeinschaft (SFB 239) are gratefully acknowledged. This work has also been funded (I. B.) by Contract No. 105/95 of the Charles University.

[1] V. M. Kenkre, in *Exciton Dynamics in Molecular Crystals and Aggregates*, edited by G. Höhler, Springer Tracts in Modern Physics, Vol. 94 (Springer, Berlin, 1982), p. 1.
[2] P. Reineker, in *Exciton Dynamics in Molecular Crystals and Aggregates*, edited by G. Höhler, Springer Tracts in Modern Physics, Vol. 94 (Springer, Berlin, 1982), p. 111.
[3] H. Haken and P. Reineker, in *Excitons, Magnons and Phonons in Molecular Crystals*, edited by A. B. Zahlan (Cambridge University Press, Cambridge, England, 1968), p. 185.
[4] V. M. Kenkre and R. S. Knox, Phys. Rev. B **9**, 5279 (1974).
[5] V. Čápek and I. Barvík, J. Phys. C **18**, 6149 (1985).
[6] M. K. Grover and R. Silbey, J. Chem. Phys. **52**, 2099 (1969).
[7] H. Haken and G. Strobl, in *The Triplet State*, edited by A. B. Zahlan (Cambridge University Press, Cambridge, England, 1967).
[8] H. Haken and P. Reineker, Z. Phys. **249**, 253 (1972).
[9] H. Haken and G. Strobl, Z. Phys. **262**, 135 (1973).
[10] Y. Inaba, J. Phys. Soc. Jpn. **52**, 3144 (1983).
[11] K. Kassner and P. Reineker, Z. Phys. B **59**, 357 (1985).
[12] K. Kassner and P. Reineker, Z. Phys. B **60**, 87 (1985).
[13] K. Kassner, Z. Phys. B **70**, 229 (1988).
[14] B. Kaiser, A. M. Jayannavar, and P. Reineker, J. Lumin. **43**, 73 (1989).
[15] V. Kraus and P. Reineker, Phys. Rev. A **43**, 4182 (1991).
[16] Ch. Warns, Diplomarbeit, Universität Ulm, 1992.
[17] V. E. Shapiro and V. Loginov, Physica A **91**, 563 (1978).
[18] B. W. Char, K. O. Geddes, G. H. Gonnet, B. L. Leong, M. B. Monagan, and S. M. Watt, *MAPLE Reference Manual* (Springer-Verlag, New York, 1991).
[19] Upon request, the analytical expressions derived with MAPLE can be obtained from P. Reineker as a LaTeX file.